CZECH TECHNICAL UNIVERSITY IN PRAGUE

FAKULTY OF ELECTRICAL ENGINEERING

DEPARTMENT OF RADIOELECTRONICS

STUDY OF NEAR-FIELD ACOUSTIC HOLOGRAPHY METHODS ON MODELS

BACHELOR THESIS

AUTOR: SVETLANA LUKIANOVA
SUPERVISOR: PROF. ING. ONDŘEJ JIŘÍČEK, CSC

STUDY PROGRAM: COMMUNICATIONS, MULTIMEDIA, ELECTRONICS
BRANCH OF STUDY: MULTIMEDIA TECHNOLOGY

PRAGUE, MAY 2019

Declaration

I declare that I have completed the presented thesis independently and that I wrote down all the used sources in accordance with the methodological instruction on ethical principles in academic theses.

In Prague, 24. May 2019

Prohlášení

Prohlašuji, že jsem předloženou práci vypracoval samostatně a že jsem uvedl veškeré použité informační zdroje v souladu s Metodickým pokynem o dodržovaní etických principů při přípravě vysokoškolských závěrečných prací.

V Praze dne 24. května 2019

Abstract

This bachelor thesis focuses on study of near-field acoustic holography methods and appropriate regularization technics, with following simulation of SONAH method in MATLAB. In this thesis, Tikhonov regularization is technics studied. Two ways of determination of the regularization parameter were compared: manually chosen value of the parameter and Morozov method.

Abstract

Tato bakalářská práce se zabývá rozborem metod akustické holografie v blízkém poli a vhodných regularizačních technik s následnou simulaci metody SONAH v prostředí MATLAB. V této práci je rozebraná Tichonovova regularizační metoda. Jsou porovnávané dvě metody určení regularizačního parametru: ručně zvolena hodnota a Morozovova metoda.

Keywords

Near-field acoustic holography, plane waves, sound field, NAH, SONAH, HELS, regularization, Tikhonov regularization, Morozov principle.

Klíčová slova

Akustická holografie v blízkém poli, rovinné vlny, zvukové pole, NAH, SONAH, HELS, regularizace, Tichonovova regularizace, Morozovova metoda.

ZADÁNÍ BAKALÁŘSKÉ PRÁCE

I. OSOBNÍ A STUDIJNÍ ÚDAJE

Příjmení: **Lukianova** Jméno: **Svetlana** Osobní číslo: **439558**

Fakulta/ústav: **Fakulta elektrotechnická**

Zadávající katedra/ústav: **Katedra radioelektroniky**

Studijní program: **Komunikace, multimédia a elektronika**

Studijní obor: **Multimediální technika**

II. ÚDAJE K BAKALÁŘSKÉ PRÁCI

Název bakalářské práce:

Studium metod akustické holografie v blízkém poli na modelech

Název bakalářské práce anglicky:

Study of Near-Field Acoustic Holography Methods on Models

Pokyny pro vypracování:

Proveďte rozbor metod akustické holografie v blízkém poli a následně proveďte testování zvolené metody pomocí simulace na modelovém zdroji. Zaměřte se na implementaci metod v prostředí Matlab včetně regularizačních technik. Diskutujte vliv šumu na výsledek rekonstrukce zvukového pole.

Seznam doporučené literatury:

[1] Williams, E. G.: Fourier Acoustics, Sound Radiation and Nearfield Acoustical Holography, Academic Press, 1999.
[2] Wang, Z., Wu, S.F.: Helmholtz equation–least-squares method for reconstructing the acoustic pressure field. The Journal of the Acoustical Society of America 102(4), 2020-2032, 1997.
[3] Hald, J.: Basic theory and properties of statistically optimized near-field acoustical holography. The Journal of the Acoustical Society of America 125(4), 2105- 2120, 2009.

Jméno a pracoviště vedoucí(ho) bakalářské práce:

prof. Ing. Ondřej Jiříček, CSc., katedra fyziky FEL

Jméno a pracoviště druhé(ho) vedoucí(ho) nebo konzultanta(ky) bakalářské práce:

Datum zadání bakalářské práce: **12.02.2019** Termín odevzdání bakalářské práce: **24.05.2019**

Platnost zadání bakalářské práce: **20.09.2020**

prof. Ing. Ondřej Jiříček, CSc. podpis vedoucí(ho) práce	prof. Mgr. Petr Páta, Ph.D. podpis vedoucí(ho) ústavu/katedry	prof. Ing. Pavel Ripka, CSc. podpis děkana(ky)

III. PŘEVZETÍ ZADÁNÍ

Studentka bere na vědomí, že je povinna vypracovat bakalářskou práci samostatně, bez cizí pomoci, s výjimkou poskytnutých konzultací.
Seznam použité literatury, jiných pramenů a jmen konzultantů je třeba uvést v bakalářské práci.

Datum převzetí zadání Podpis studentky

Contents

1. Introduction

Measurement of vibration and noise levels are one of the basic measurements of nonelectrical quantities. Classical method of measuring vibration using accelerometer possesses several faults. Difficulties with placement and fixation of the sensors to the source of vibration is one of them. Weight of the sensors influence the original behavior of measured objects in case of light thin plates [3],[6]. Therefore, new methods were needed.

Near-field Acoustic Holography (NAH) is a contactless method of reconstruction vibration (noise) source's quantities by measuring acoustic field in proximity to the source. This method appeared in 1980 and is based on theory of acoustic holography, which started to develop in mid 1960s [9]. Acoustic holography can be used for localization, identification and prediction of noise sources [7]. Due to taking into consideration evanescent waves, a reconstruction image with high resolution can be obtained by using NAH. One of the practical restrictions of NAH is a requirement of significant number of microphones for measurement for desired level of resolution.

The thesis are focused on study of near-field acoustic holography methods and appropriate regularization technics. Study is based on simulation of SONAH (Statistically optimized NAH) method in MATLAB. In this thesis, Tikhonov regularization is technics studied. Two ways of determination of the regularization parameter were compared: manually chosen value of the parameter and Morozov method.

2. Theoretical part

In this chapter a brief review of essential acoustic equations needed for Nearfield Acoustic Holography methods are presented.

2.2 Basic acoustic equations

One of the most important equations in acoustics is a acoustic wave equation. For a homogeneous fluid with no viscosity it defined as

$$\nabla^2 p - \frac{1}{c^2}\frac{\partial^2 p}{\partial t^2} = 0, \qquad (1)$$

where $p(x, y, z, t)$ is an acoustic pressure function, that satisfies Eq. (1), c is a constant and refers to the speed of sound in the medium (at 20°C c = 343 m/s in air and 1481 m/s in water).

In the frequency domain acoustic wave equation is defined as

$$\nabla^2 p + k^2 p = 0, \qquad (2)$$

also known as Helmholtz equation, where $k = \omega/c$ is the acoustic wave number and the frequency is $2\pi f = \omega$.

In Cartesian coordinates Laplacian operator is defined as

$$\nabla^2 \equiv \frac{\partial^2}{\partial x^2} + \frac{\partial^2}{\partial y^2} + \frac{\partial^2}{\partial z^2}.$$

Equation, that defines relation between acoustic pressure and acoustic velocity, is Euler's equation

$$\rho_0 \frac{\partial \vec{v}}{\partial t} = -\vec{\nabla} p, \qquad (3)$$

where $\vec{v} = \dot{u}\vec{\imath} + \dot{v}\vec{\jmath} + \dot{w}\vec{k}$ represents the velocity vector, where $\dot{u}, \dot{v}\ and\ \dot{w}$ are components of velocity vector.

In the frequency domain Eq. (2) becomes

$$\mathrm{i}\omega\rho_0\vec{v} = \vec{\nabla} p. \qquad (4)$$

Gradient $\vec{\nabla}$ in Cartesian coordinates is defined as

$\vec{\nabla} \equiv \frac{\partial}{\partial x}\vec{\imath} + \frac{\partial}{\partial y}\vec{\jmath} + \frac{\partial}{\partial z}\vec{k},$

where $\vec{\imath}$, $\vec{\jmath}$, $\vec{k}$ are unit vectors in x, y and z directions respectively.

Next let us introduce sound intensity. In time domain sound intensity is defined as

$$\vec{I}(t) = p(t)\,\vec{v}\,(t). \tag{5}$$

Problematic places are determined by large levels of sound intensity.

Sound energy density in steady state in source-free region is [9]

$$\vec{\nabla}\cdot\vec{I}(\omega) = 0, \tag{6}$$

where

$$\vec{I}(\omega) = \frac{1}{T}\int_0^T p(t)\,\vec{v}\,(t)\mathrm{d}t, \tag{7}$$

or using complex variable notation

$$\vec{I}(\omega) = \frac{1}{2}Re(p(\omega)\,\vec{v}\,(\omega)^*). \tag{8}$$

$T = 1/f$, f is a excitation frequency.

Eq. (6) means that in source-free region the divergence of the time average acoustic intensity must be 0. The divergence could be not 0 only when there are energy loses in medium or if there is a source in the referred area.

2.3 Plane waves

The general equation describing plane wave in the frequency domain is [9]

$$p(\omega) = A(\omega)\mathrm{e}^{\mathrm{i}(k_x x + k_y y + k_z z)}\quad, \tag{9}$$

where $A(\omega)$ is an arbitrary constant, and

$$k^2 = k_x^2 + k_y^2 + k_z^2. \tag{10}$$

The general plane wave in time domain at the frequency ω_0 is described by equation [9]

$$p(t) = A\mathrm{e}^{\mathrm{i}(k_x x + k_y y + k_z z - \omega_0 t)}, \tag{11}$$

where *A* is an arbitrary constant and $k = \omega_0/c$.

A plane wave can be represented using condensed notation [9]:

$$\mathrm{e}^{\mathrm{i}(k_x x + k_y y + k_z z)} = \mathrm{e}^{\mathrm{i}(\vec{k}\cdot\vec{r})}, \tag{12}$$

where $\vec{r}$ represent the position vector to the observation point in the sound field, and $\vec{k}$ gives the direction of the wave [9].

The particle velocity of plane wave in the frequency domain, given by Eq. (4) and Eq. (9), is defined as

$$\vec{v}(\omega) = \frac{1}{\mathrm{i}\omega\rho_0}(k_x\vec{\imath} + k_y\vec{\jmath} + k_z\vec{k})p(\omega). \tag{13}$$

Since k is a constant and k_x, k_y, k_z are not independent of one another, usually k_z is chosen as dependent variable, with k_x *and* k_y as independent ones, so

$$k_z^2 = k^2 - k_x^2 - k_y^2,$$

$$k_z = \pm\sqrt{k^2 - k_x^2 - k_y^2}. \tag{14}$$

When k_x or $k_y > k$, plane wave turns into evanescent wave. Then Eq. (14) becomes

$$k_z = \pm\mathrm{i}\sqrt{k^2 - k_x^2 - k_y^2} = \pm\mathrm{i}\, k_z', \tag{15}$$

where k_z' is real, and the plane wave, turned evanescent, has the form [9]

$$p = A\mathrm{e}^{-k_z' z}\mathrm{e}^{\mathrm{i}(k_x x + k_y y)}. \tag{16}$$

This is a form of an evanescent plane wave decaying in z direction.

From Eq. (4) the particle velocity of evanescent plane wave is

$$\vec{v}(\omega) = \frac{1}{\mathrm{i}\omega\rho_0}(k_x\vec{\imath} + k_y\vec{\jmath} + k_z'\vec{k})p(\omega). \tag{17}$$

2.4 Nearfield acoustic holography

2.4.1 Fourier based NAH

The oldest method of NAH, based on measurement across a surface in separable coordinate system, allowing calculation to be performed by spatial discrete Fourier transform (DFT) or fast Fourier transform (FFT) [2].

The pressure in source-free region can be described completely by sum of plane and evanescent waves [9].

$$p(x, y, z) = \sum_{k_x}\sum_{k_y} P(k_x, k_y)\,\mathrm{e}^{\mathrm{i}(k_x x + k_y y + k_z z)}, \tag{18}$$

where k_x and k_y are independent variables, k_z depends on them. $P(k_x, k_y)$ is multiplying coefficient, depending on two wavenumbers.

For a general problem [9]

$$p(x, y, z) = \frac{1}{4\pi^2} \int_{-\infty}^{\infty} \mathrm{d}k_x \int_{-\infty}^{\infty} \mathrm{d}k_y P(k_x, k_y)\, \mathrm{e}^{\mathrm{i}(k_x x + k_y y + k_z z)} \tag{19}$$

If $z = 0$ Eq. (19) becomes

$$p(x, y, 0) = \frac{1}{4\pi^2} \int_{-\infty}^{\infty} \mathrm{d}k_x \int_{-\infty}^{\infty} \mathrm{d}k_y P(k_x, k_y)\, \mathrm{e}^{\mathrm{i}(k_x x + k_y y)}, \tag{20}$$

and represent a pressure in the infinite plane at $z = 0$.

Comparing Eq. (19) to a definition of inverse Fourier transform, is clear that the complex amplitude $P(k_x, k_y)$ can be defined as

$$P(k_x, k_y) = \int_{-\infty}^{\infty} \mathrm{d}x \int_{-\infty}^{\infty} \mathrm{d}y\, p(x, y, 0)\, \mathrm{e}^{-\mathrm{i}(k_x x + k_y y)}. \tag{21}$$

$P(k_x, k_y)$ is called the angular spectrum [9].

After determination of the angular spectrum, we can determinate the pressure field in 3D space using Eq. (19).

The general expression to extrapolate the angular spectrum in the plane z' to the plane z is [9]

$$P(k_x, k_y, z) = P(k_x, k_y, z')\mathrm{e}^{\mathrm{i}k_z(z - z')}, \tag{22}$$

with the assumption, that

$$P(k_x, k_y) = P(k_x, k_y, 0). \tag{23}$$

Using Eq. (4) we can calculate three angular spectrum components of the velocity vector

$$\dot{U}(k_x, k_y, z)\vec{\imath} + \dot{V}(k_x, k_y, z)\vec{\jmath} + \dot{W}(k_x, k_y, z)\vec{k} = \frac{1}{\rho_0 c k}(k_x\vec{\imath} + k_y\vec{\jmath} + k_z\vec{k})P(k_x, k_y, z), \tag{24}$$

where $\dot{W}(k_x, k_y, z)$ is a two-dimensional Fourier transform of a velocity vector's component $\dot{w}(x, y, z)$

$$\dot{W}(k_x, k_y, z) = \mathcal{F}_x\mathcal{F}_y[\dot{w}(x, y, z)]\,. \tag{25}$$

Analogically with $\dot{U}(k_x, k_y, z)\ and\ \dot{V}(k_x, k_y, z)$.

Using Eq. (24) and Eq. (22) we can relate the velocity to the pressure in a different plane [9]

$$\dot{U}(k_x, k_y, z)\vec{\imath} + \dot{V}(k_x, k_y, z)\vec{\jmath} + \dot{W}(k_x, k_y, z)\vec{k} = \frac{1}{\rho_0 c k}(k_x\vec{\imath} + k_y\vec{\jmath} + k_z\vec{k})P(k_x, k_y, z')e^{\mathrm{i}k_z(z - z')}. \tag{26}$$

Then the normal component of velocity is

$$\dot{W}(k_x, k_y, z) = \frac{k_z}{\rho_0 ck} P(k_x, k_y, z') e^{\mathrm{i}k_z(z-z\prime)}. \tag{27}$$

Eq. (27) relates the angular spectrum components of normal velocity in one plane to the components of pressure in a different plane [9].

The Rayleigh's second integral relates the spatial pressure in one plane to the spatial pressure in another plane, with $z \geq z'$, [9]

$$p(x, y, z) = -\frac{1}{2\pi} \int_{-\infty}^{\infty} \int_{-\infty}^{\infty} p(x', y', z') \frac{\partial}{\partial z'} \left[\frac{\mathrm{e}^{\mathrm{i}k|\vec{r}-\vec{r}\prime|}}{|\vec{r} - \vec{r}'|} \right] \mathrm{d}x' \mathrm{d}y', \tag{28}$$

where $\vec{r} = (x, y, z)$, $\vec{r}' = (x', y', z')$, and

$$|\vec{r} - \vec{r}'| = \sqrt{(x - x')^2 + (y - y')^2 + (z - z')^2}$$

The Rayleigh's first integral relates the spatial pressure in one plane to the normal component of the velocity in another plane, with $z \geq z'$,

$$p(x, y, z) = -\frac{\mathrm{i}\rho_0 ck}{2\pi} \int_{-\infty}^{\infty} \int_{-\infty}^{\infty} \dot{w}(x', y', z') \frac{\partial}{\partial z'} \left[\frac{\mathrm{e}^{\mathrm{i}k|\vec{r}-\vec{r}\prime|}}{|\vec{r} - \vec{r}'|} \right] \mathrm{d}x' \mathrm{d}y'. \tag{29}$$

Both Rayleigh's integrals provide means to compute the radiation into half space $z \geq z'$ using the information of the pressure on a surface $z = z'$, Eq. (28), or the normal velocity on a plane $z = z'$, Eq. (29) and provide solution only for a forward problem. In other words, they can only provide the pressure radiated from the sources [9]. For inverse problems solution is provided by NAH.

The mathematics behind NAH is summarized in the single statement [9]

$$\dot{w}(x, y, z_h) = \mathcal{F}_x^{-1} \mathcal{F}_y^{-1} [\mathcal{F}_x \mathcal{F}_y [p(x, y, z_h)] G(k_x, k_y, z_s - z_h)], \tag{30}$$

where $z = z_s$ is a surface of the vibration source, $z = z_h$ is a measurement plane, and $z_s \leq z_h$.

G is called the velocity propagator and is defined as

$$G(k_x, k_y, z - z_h) \equiv \frac{k_z}{\rho_0 ck} \mathrm{e}^{\mathrm{i}k_z(z-z_h)}. \tag{31}$$

Using the convolution theorem, Eq. (30) can be rewritten as [9]

$$\dot{w}(x, y, z_s) = p(x, y, z_h) ** g_v^{-1}(x, y, z_s - z_h), \tag{32}$$

where symbol $**$ represent a two-dimensional convolution, and $g_v^{-1}(x, y, z_s - z_h)$ is the inverse velocity propagator defined as [9]

$$\begin{aligned} g_v^{-1}(x, y, z_s - z_h) &\equiv \mathcal{F}_x^{-1} \mathcal{F}_y^{-1} [G(k_x, k_y, z_s - z_h)] \\ &= \mathcal{F}_x^{-1} \mathcal{F}_y^{-1} \left[\frac{k_z}{\rho_0 ck} \mathrm{e}^{\mathrm{i}k_z(z-z_h)} \right] \end{aligned} \tag{33}$$

Because NAH solves the inverse problem, the mathematical solution must be unique and stable. And therefore Eq. (30) must be approached with caution.
DFT and FFT are needed for discretization of the holography equation, for any practical measurement.
The final holography equation would be [9]

$$\widetilde{w}_D(x,y,z_s) = \sum_{p,q=-\infty}^{\infty} p_D(x - L_x, y - L_y, z_h) ** \mathcal{F}_x^{-1}\mathcal{F}_y^{-1}[G], \tag{34}$$

where p_D is a sampled version of the measured pressure p over the measured aperture and is zero outside of it and must be dense enough to avoid aliasing [9], L_x and L_y are dimensions of the aperture.
The inverse propagator operates on an infinite plane of replicated measurements, not just an actual one. The replicated measurements outside the actual one are reconstructed in the same way as the actual measurement aperture by convolution with the inverse propagator, but this measurements contribute less to the velocity in the reconstructed aperture because they are further from it. Since the left side of Eq. (34) is periodic, the reconstructed sources also form an infinite grid of replicated apertures, called replicated sources [9].
The simplest way to reduce the errors due to replicated measurements is to add zeros outside the actual measurement, to at least double the size of the measured aperture. The improvement is obtained through the increased distance between the replicated pressure measurement and the corresponding reduction in their influence in the reconstruction over the real source[9].
The use of DFT allows NAH to proceed data very fast but appears a side-effect in form of a spatial windowing effect, unless the measurement fully covers the area with high sound pressure. In some cases this requirement cannot be fulfilled, and in many cases the necessary size becomes prohibitively large [2].

2.4.2 Statistically optimized NAH (SONAH)

SONAH was developed to overcome limitations of Fourier based NAH [2]. Prediction of particle velocity and acoustic pressure directly in time domain allows to avoid using Fourier transform [1].

SOHAN use a local model of the sound field in terms of elementary wave functions and perform fit of the elementary wave model (EWM) to the measured sound field data [2].

The matrix SONAH formulation is

$$\mathbf{Ba} = \mathbf{p}, \tag{35}$$

where

$$\mathbf{B} = \{\psi_{\boldsymbol{n}}(\boldsymbol{r}_i)\} = \begin{Bmatrix} \psi_{\mathbf{1}}(\boldsymbol{r}_1) & \psi_{\mathbf{2}}(\boldsymbol{r}_1) & \cdots & \psi_{\boldsymbol{N}}(\boldsymbol{r}_1) \\ \psi_{\mathbf{1}}(\boldsymbol{r}_{\mathbf{2}}) & \psi_{\mathbf{2}}(\boldsymbol{r}_{\mathbf{2}}) & & \psi_{\boldsymbol{N}}(\boldsymbol{r}_2) \\ \vdots & & \ddots & \vdots \\ \psi_{\mathbf{1}}(\boldsymbol{r}_I) & \psi_{\mathbf{2}}(\boldsymbol{r}_I) & \cdots & \psi_{\boldsymbol{N}}(\boldsymbol{r}_I) \end{Bmatrix}, \tag{36}$$

$\mathbf{B}$ is a matrix of values of wavefunctions ψ at the measurements positions $\boldsymbol{r}_i$, i=1, 2, …, I, in a source-free area.

$$\mathbf{p} = \{p(\boldsymbol{r}_i)\} = \begin{Bmatrix} p(\boldsymbol{r}_1) \\ p(\boldsymbol{r}_2) \\ \vdots \\ p(\boldsymbol{r}_I) \end{Bmatrix}, \tag{37}$$

is a vector of measured pressures.

$$\mathbf{a} = \{a_n\} = \begin{Bmatrix} a_1 \\ a_2 \\ \vdots \\ a_N \end{Bmatrix}, \tag{38}$$

is a vector of the complex expansion coefficients.

Because of the ill-posed nature of the inverse problem, regularization is needed.

General SONAH formulation of estimated sound pressure $\tilde{p}(\boldsymbol{r})$, including regularization[2]:

$$\tilde{p}(\boldsymbol{r}) = \widetilde{\boldsymbol{a}}^T \boldsymbol{\alpha}(\boldsymbol{r}) = \boldsymbol{p}^T[(\mathbf{BB}^H + \varepsilon\mathbf{I})^{-1}]^T \mathbf{B}^* \boldsymbol{\alpha}(\boldsymbol{r}) =$$
$$= \boldsymbol{p}^T[(\mathbf{BB}^H + \varepsilon\mathbf{I})^T]^{-1} \mathbf{B}^* \boldsymbol{\alpha}(\boldsymbol{r}) = \tag{39}$$
$$= \boldsymbol{p}^T[\mathbf{A}^H\mathbf{A} + \varepsilon\mathbf{I}]^{-1}\mathbf{A}^H \boldsymbol{\alpha}(\boldsymbol{r}) = \mathbf{p}^T\mathbf{c}(\mathbf{r}).$$

Where $\mathbf{A} = \mathbf{B}^T$, and $\widetilde{\boldsymbol{a}}$ is a coefficient vector estimated from the measurement.

$\mathbf{I}$ is a unit diagonal matrix of appropriate dimensions, ε is a regularization parameter.

Symbols T representing transpose of a matrix or a vector, symbol H represents Hermitian transpose and symbol $*$ represents complex conjugate.

Matrix $\boldsymbol{A}^H\boldsymbol{A}$ can be perceived as matrix of cross correlations between the measurement points in the domain of the elementary wave functions and can be defined as [2]

$$[\boldsymbol{A}^H\boldsymbol{A}]_{ij} = \sum_n \psi_n^*(\mathrm{r}_i)\psi_n(r_j). \quad (40)$$

Vector $\mathbf{A}^H\boldsymbol{\alpha}(\boldsymbol{r})$ then contains the cross correlations between the measurement points and the estimation position and can be defined as [2]

$$[\mathbf{A}^H\boldsymbol{\alpha}(\boldsymbol{r})]_i = \sum_n \psi_n^*(\mathrm{r}_i)\psi_n(r). \quad (41)$$

Then the estimated particle velocity in a χ direction is [2]

$$\tilde{u}_\chi(\boldsymbol{r}) = -\frac{1}{i\omega\rho_0}\frac{\partial\tilde{p}(\boldsymbol{r})}{\partial\chi} \quad (42)$$

Here ω is the angular frequency, ρ_0 is the density of the medium.

2.4.3 Helmholtz equation least-squares method (HELS)

When using HELS method, the reconstruction of the acoustic field is done by directly solved the Helmholtz equation, Eq. (2). The acoustic pressure is expanded in terms of a set of independent functions ψ^*, that are generated by the Gram-Schmidt orthonormalization with respect to the solution of the Helmholtz equation on the actual vibrating plane [8]. The coefficients of these functions are determined by requiring form of the solution to satisfy the boundary conditions of the measurement [8].

The solution of the Helmholtz equations, with respect to boundary conditions, can be approximated by a linear combination of the functions ψ^*

$$p^* = \rho c \sum_{i=1}^{N} C_i\psi_i^*. \quad (43)$$

Where ρ is the density of the medium, c is the speed of sound in the medium, C_i are the coefficients.

After determination of C_i, the acoustic pressure can be approximated anywhere using Eq. (43) [8].

Suppose that an N -term expansion used in Eq. (43) and M measurements is taken ($N \leq M$), than

$$\begin{Bmatrix} \psi_{11}^* & \psi_{12}^* & \cdots & \psi_{1N}^* \\ \psi_{21}^* & \psi_{22}^* & & \psi_{2N}^* \\ \vdots & \vdots & \ddots & \vdots \\ \psi_{1N}^* & \psi_{2N}^* & & \psi_{3N}^* \\ \vdots & \vdots & \ddots & \vdots \\ \psi_{M1}^* & \psi_{M2}^* & \cdots & \psi_{MN}^* \end{Bmatrix} \begin{Bmatrix} C_1 \\ C_2 \\ \vdots \\ C_N \end{Bmatrix} = \begin{Bmatrix} p_{01} \\ p_{02} \\ \vdots \\ p_{0N} \\ \vdots \\ p_{0M} \end{Bmatrix} \tag{44}$$

If the measured quantities p_0 are exact, then the approximated solution p^* converges to the true value as $N \to \infty$ [8].

The coefficients C_i can be solved [8]

$$\mathbf{C} = \frac{1}{\rho c} \boldsymbol{\mathcal{T}}^{\mu} \mathbf{p}_0, \tag{45}$$

where $\boldsymbol{\mathcal{T}}$ is a transformation matrix, and $\boldsymbol{\mathcal{T}}^{\mu}$ is pseudoinverse transformation matrix and define as [8]

$$\boldsymbol{\mathcal{T}}^{\mu} = ([\psi_{mn}^*]^T [\psi_{mn}^*])^{-1} [\psi_{mn}^*]^T, \tag{46}$$

where $[\psi_{mn}^*]$ represent a matrix of the same form as a matrix of ψ^* in Eq. (44).

2.5 Regularization

Due to existence of the evanescent waves in near-field, that decay at various rates, the inverse problems are usually ill-posed. Regularization provides a technics to overcome the ill-posedness [10].

2.5.1 Tikhonov regularization

Tikhonov regularization is one of the most used regularization technics.

In the Tikhonov regularization method we have to minimize, with respect to $\dot{w}$ for a fixed parameter α, the general Tikhonov function J_α given by [10]

$$J_\alpha(\dot{w}^\delta) = \left\|\mathbf{H}\dot{w}^\delta - p^\delta\right\|^2 + \alpha\left\|\mathbf{L}\dot{w}^\delta\right\|^2, \tag{47}$$

where $\|.\|$ represent the L2 norm, usually $\mathbf{L} = \mathbf{I}$, where $\mathbf{I}$ is a unit diagonal matrix of needed size, p^δ is the pressure data with noise, $\mathbf{H}$ is a spatial transfer function with the dimension $M \times M$, which directly relates the pressure vector to the velocity vector. The $\alpha\left\|\mathbf{L}\dot{w}^\delta\right\|^2$ is so called penalty term, in this case it prevents the amplitude of the reconstructed normal velocity from growing without a limit during the minimalization [10].

The solution, $\dot{w}^{\alpha,\delta}$, for the minimalization of Eq. (47), is given by[10]:

$$\dot{w}^{\delta} = \dot{w}^{\alpha,\delta} = \mathbf{R}_{\boldsymbol{\alpha}} p^{\delta}, \tag{48}$$

Where $\mathbf{R}_{\boldsymbol{\alpha}}$ is a regularized inverse of $\mathbf{H}$,

$$\mathbf{R}_{\boldsymbol{\alpha}} = (\boldsymbol{\alpha}\mathbf{L}^{H}\mathbf{L} + \mathbf{H}^{H}\mathbf{H})^{-\mathbf{1}}\mathbf{H}^{H} = (\boldsymbol{\alpha}\mathbf{I} + \mathbf{H}^{H}\mathbf{H})^{-\mathbf{1}}\mathbf{H}^{H}, \boldsymbol{for\ \alpha > 0}. \tag{49}$$

For determination of parameter $\boldsymbol{\alpha}$ could be used several methods.

First, for the sake of mentioning, coefficient $\boldsymbol{\alpha}$ can be chosen manually. The disadvantage of this method is, that the form of the reconstructed sound field is very sensitive to $\boldsymbol{\alpha}$, and could differ dramatically with different values of $\boldsymbol{\alpha}$.

Next one, the Morozov discrepancy principle. This is a simple method for finding the regularization parameter when is known the variance of the noise σ^2.

The Morozov discrepancy principle states that the solution for Eq. (47) must satisfy the equation [10]:

$$\left\|\mathbf{H}\dot{w}^{\alpha,\delta} - p^{\delta}\right\|^{2} = \delta,\ \ \delta = \sqrt{M}\sigma. \tag{50}$$

or

$$p^{\alpha,\delta} \equiv \mathbf{H}\dot{w}^{\alpha,\delta} = \mathbf{H}\mathbf{R}_{\boldsymbol{\alpha}} p^{\delta}. \tag{51}$$

We vary the $\boldsymbol{\alpha}$, and thus $\mathbf{R}_{\boldsymbol{\alpha}}$, in Eq. (49), until the predicted pressure differs from the measured pressure by just the noise [10].

2.5.2 Landweber iteration

Using this technic, we have [10]

$$\dot{w} = (I - \beta\mathbf{H}^{H}\mathbf{H})\dot{w} + \beta\mathbf{H}^{H}p, \tag{52}$$

where β is a positive number to be determined.

The iteration procedure is set up by using the right side to compute the left side starting with the first iteration of $\dot{w}^{0} = 0$ [10]. Than

$$\dot{w}^{m} = (I - \beta\mathbf{H}^{H}\mathbf{H})\dot{w}^{m-1} + \beta\mathbf{H}^{H}p, \qquad m = 1, 2, \ldots \tag{53}$$

For convergence, β must be chosen less than $1/|\lambda_{max}|^2$

3. Practical part

In this part of the thesis the simulation of the SONAH method is described and discussed and two methods of determination of the regularization parameter are compared.

3.2 Simulation description

The simulations were realized in MATLAB, therefore the description of the simulation steps is presented in the form of MATLAB code. The first step in trying to recreate sound field in forward and inverse directions is to define the source(s) of sound.

In this simulation the tree sources on different coordinates were chosen:

```
%%source's positions
% source 1
x1=0.4;
y1=0.2;

%source 2
x2=0.8;
y2=0.55;

%source 3
x3=0.5;
y3=0.65;
```

For the source the same characteristics were used:

```
f=1000; %Hz frequency
A1=1; %amplitude
w=2*pi*f; % angular speed
lambda=c/f; %m wave length
k0=w/c; %wave number
```

Than the basic properties of the surrounding medium were defined:

```
c=343; %m/s speed of sound in air
pref=2*10^-5; %Pa
p0=1.275; %kg/m3 air density
```

Finally the aperture size with the coordinates of the measured points was set:

```
%aperture
x=linspace(1,0,40);
y=linspace(1,0,40);
```

If it was the actual measurement, then in these points the microphones for the sound pressure measurements would be placed.

Then for each source we determine the matrix of the distances from the source to the measured point:

```
%distance matrix, source plane
for m=1:length(y)
   for n=1:length(x)
      r1source(m,n)=sqrt((x(n)-x1)^2+(y(m)-y1)^2);
      r2source(m,n)=sqrt((x(n)-x2)^2+(y(m)-y2)^2);
      r3source(m,n)=sqrt((x(n)-x3)^2+(y(m)-y3)^2);
   end
end
```

The same principle for the distance matrix for the measurement plane and the reconstruction plane is used, with respect to the z coordinate. For the measurement plane it is $\lambda/3$ and for the reconstruction plane it is $2\lambda/3$.

The measurement plane is the plane where the actual measurement have been held. So simulated data on the measurement plane would be referred as the actual measurement data. The reconstruction plane is the plane, where the forward problem have been reconstructed, meaning radiation from the source to given distance. And the source plane is the plane where the sound sources have been located. In following text, these planes would be referred as measurement plane, reconstruction plane and source plane respectively.

For the evaluation and comparison purposes we determine the “true” sound pressure on all three planes.

```
%sount pressure on measured plane
p1meas=(A1.*exp(-j*k0.*r1meas))./r1meas; %pressure from source 1
p2meas=(A1.*exp(-j*k0.*r2meas))./r2meas; %preassure from source 2
p3meas=(A1.*exp(-j*k0.*r3meas))./r3meas; %pressure from source 3
Pm=p1meas+p2meas+p3meas; %total pressure from all three sourcec
pmeas=abs(p1meas+p2meas+p3meas); %total abs pressure without
noise, abs
Lmeas=20*log10((pmeas)/pref); %pressure level without noise
```

Similar calculations were done on other two planes.

Then we add a tree levels of white gaussian noise with selected variance and mean=0 to the measured pressure. First noise with the variance of the minimum value from all measured pressures, second noise with variance of the 10 times of this minimum value, and third noise with variance of the 20 times of this minimum value.

```
%noise definition
pmin=min(min(pmeas)); %determination of minimal pressure value
s1=pmin*1; %sqrt noise variance level 1
s2=pmin*10; %sqrt noise variance level 2
s3=pmin*20; %sqrt noise variance level 3
```

Consequently, the simulated pressure with the noise calculate:

```
pmeas_noise1=Pm + s1*randn(size(Pm)); %prassure on measured plane
with noise1
Lmeas_noise1=20*log10(abs(pmeas_noise1)/pref); %pressure level on
measured plane with noise1
pmeas_noise2=Pm + s2*randn(size(Pm)); %prassure on measured plane
with noise2
Lmeas_noise2=20*log10(abs(pmeas_noise2)/pref); %pressure level on
measured plane with noise2
pmeas_noise3=Pm + s3*randn(size(Pm)); %prassure on measured plane
with noise3
Lmeas_noise3=20*log10(abs(pmeas_noise3)/pref); %pressure level on
measured plane with noise3
```

Similar calculations are done on the other two planes.

These calculated sound pressure levels on the source plane and the reconstruction plane are used as the reference.

Now we will reconstruct the sound pressure on two planes, the source plane and the reconstruction plane, using simulated data only from the measurement plane, with the exception of the matrix $\mathbf{B}$, that is a matrix of elementary wave function values, that in this simulation can be substituted by the matrixes of the sound pressure functions without noise.

We will use the same measured data for both problems.

For the pressure on the source plane, the solution of the inverse problem is:

```
Bsource=(p1source+p2source+p3source); %matrix of Elementary Wave
Functions for source plane
Asource=Bsource.';
C=conj(Bsource);
```

```
for ii=1:length(x)
      cross_source=(C(ii).*Bsource);
end

prsource=abs((Pm.')*inv((Asource')*Asource+eps_source0*eye(length(x))*
cross_source); % without noise
prsource_noise1=abs((pmeas_noise1.')*inv((Asource')*Asource+
eps_source1*eye(length(x)))*cross_source); % with noise 1
prsource_noise2=abs((pmeas_noise2.')*inv((Asource')*Asource+
eps_source2*eye(length(x)))*cross_source); % with noise 2
prsource_noise3=abs((pmeas_noise3.')*inv((Asource')*Asource+
eps_source3*eye(length(x)))*cross_source); % with noise 3
```

And for the reconstructed plane, the solution of the forward problem can be realized as:

```
Brec=p1rec+p2rec+p3rec; %matrix of Elementary Wave Functions for
reconstructed plane
Arec=Brec.';
D=conj(Brec);
for ii=1:length(x)
       crossrec=(D(ii).*Brec);
end

prrec=abs((Pm.')*inv((Arec')*Arec+eps_rec0*eye(length(x),length(y)))*
crossrec); %without noise
prrec_noise1=abs((pmeas_noise1.')*inv((Arec')*Arec+
eps_rec1*eye(length(x)))*crossrec); % with noise 1
prrec_noise2=abs((pmeas_noise2.')*inv((Arec')*Arec+
eps_rec2*eye(length(x)))*crossrec); % with noise 2
prrec_noise3=abs((pmeas_noise3.')*inv((Arec')*Arec+
eps_rec3*eye(length(x)))*crossrec); % with noise 3
```

For the both problems the sound pressure for the noiseless simulated measured data and for the tree levels of the noisy data are reconstructed. For the both problems two methods of determination of the regularization parameter ε are used. The first one is an manually chosen positive number, and the second one is using the Morozov method.

3.3 Simulation results

The sound pressure levels of all three planes without noise are shown in the figures below.

These sound levels are simulated for reference purposes. The reconstructed sound fields must have some resemblance to these reference levels.

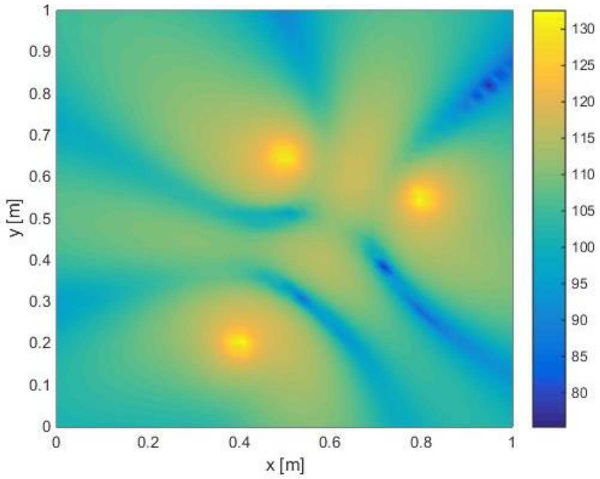

Fig. 1. The sound pressure level on the source plane, without noise

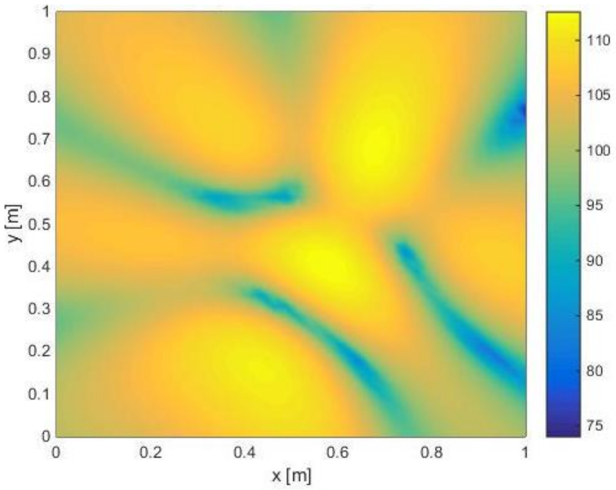

Fig. 2. The sound pressure level on the measurement plane, without noise

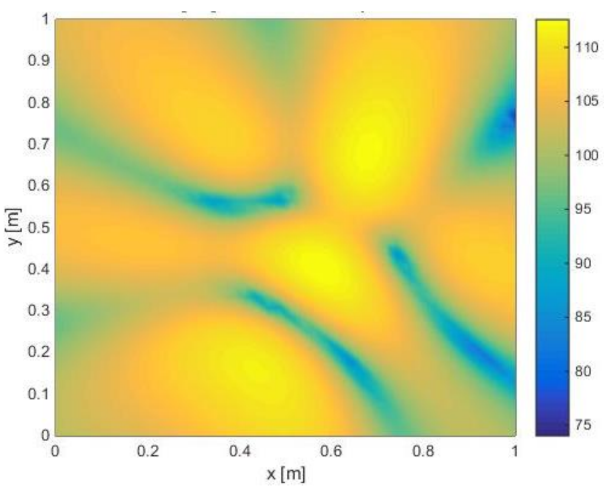

Fig. 3. The sound pressure level on the reconstruction plane, without noise

The manually chosen parameters for the reconstruction of the both planes are:

```
eps_source0=18; %regularization parameter for reconstruction without noise
eps_source1=20; %regularization parameter for reconstruction with noise1
eps_source2=35; %regularization parameter for reconstruction with noise2
eps_source3=40; %regularization parameter for reconstruction with noise3
eps_rec0=25; %regularization parameter for reconstruction without noise
eps_rec1=25; %regularization parameter for reconstruction with noise 1
eps_rec2=29; %regularization parameter for reconstruction with noise 2
eps_rec3=28; %regularization parameter for reconstruction with noise 3
```

The sound levels for these values of the regularization parameter are:

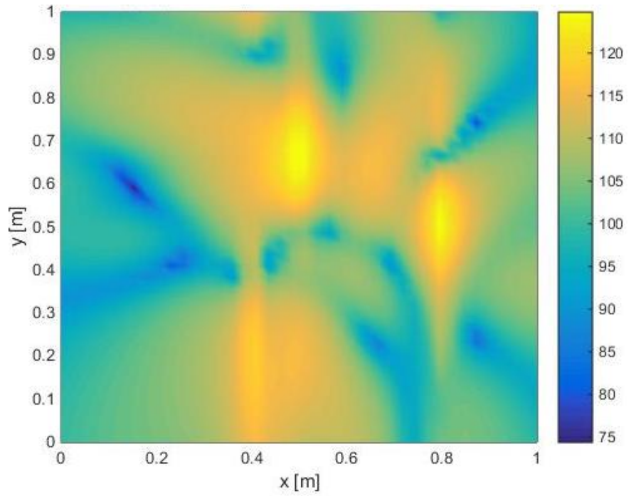

Fig. 4. The sound pressure level on the source plane, reconstructed using the SONAH general equation with manually chosen regularization parameter

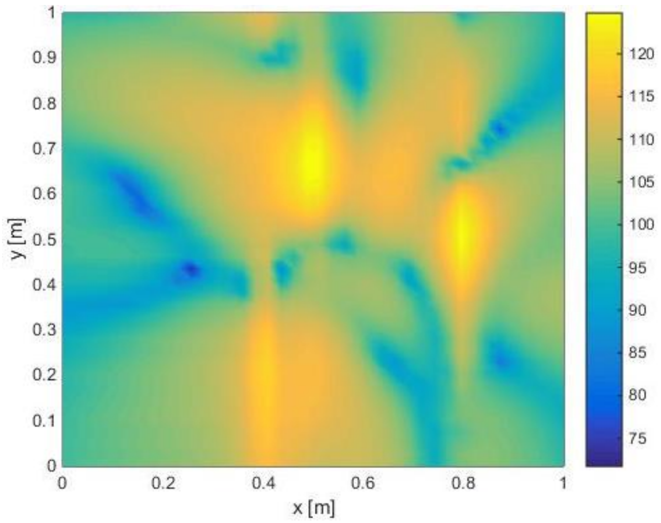

Fig. 5. The sound pressure level on the source plane with noise 1, reconstructed using the SONAH general equation with manually chosen regularization parameter

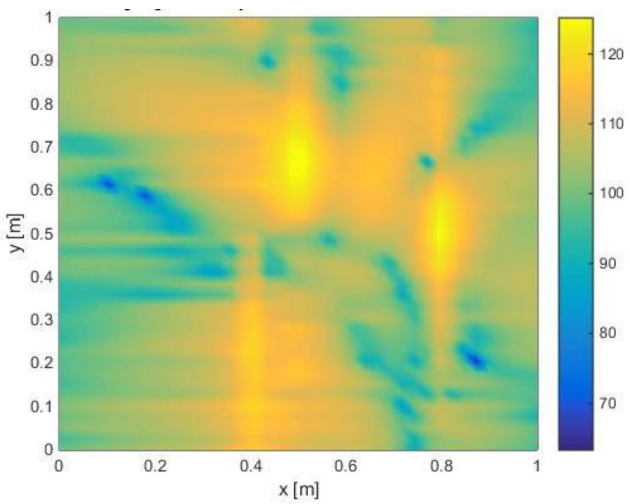

Fig. 6. The sound pressure level on the source plane with noise 2, reconstruction using the SONAH general equation with manually chosen regularization parameter

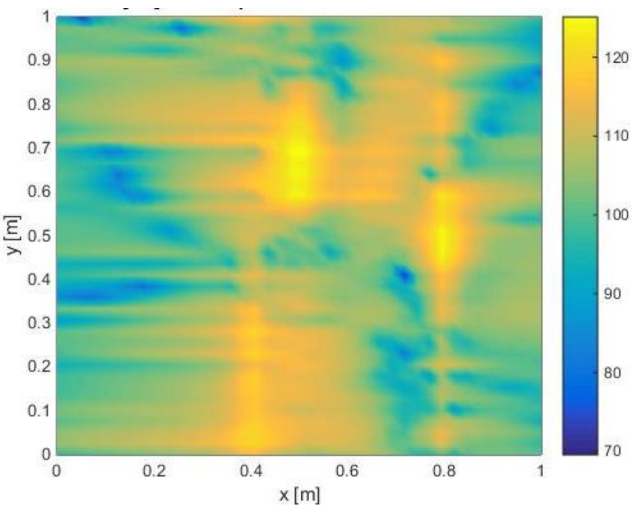

Fig. 7. The sound pressure level on the source plane with noise 3, reconstructed using the SONAH general equation with manually chosen regularization parameter

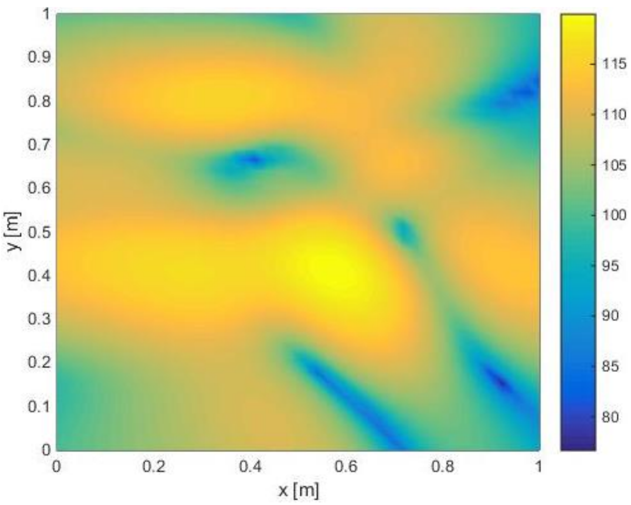

Fig. 8. The sound pressure level on the reconstruction plane, reconstructed using the SONAH general equation with manually chosen regularization parameter

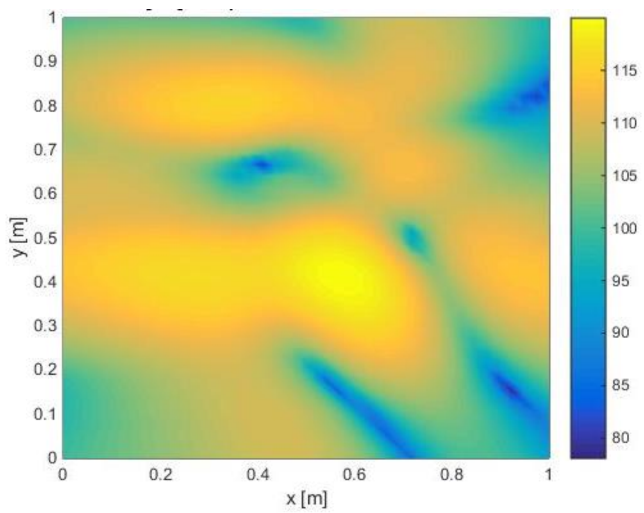

Fig. 9. The sound pressure level on the reconstruction plane with noise1, reconstructed using the SONAH general equation with manually chosen regularization parameter

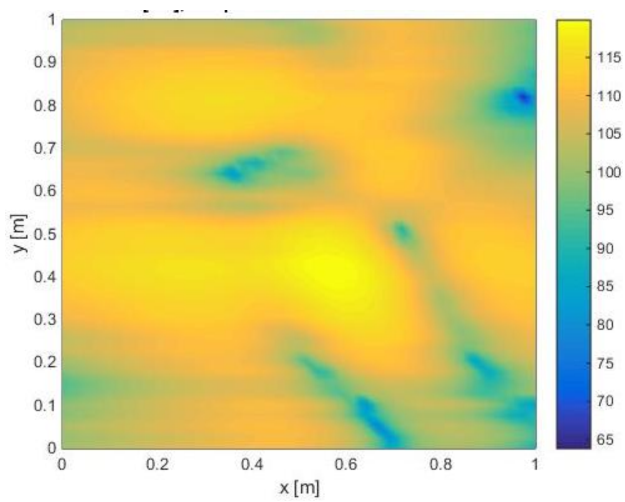

Fig. 10. The sound pressure level on the reconstruction plane with noise2, reconstructed using the SONAH general equation with manually chosen regularization parameter

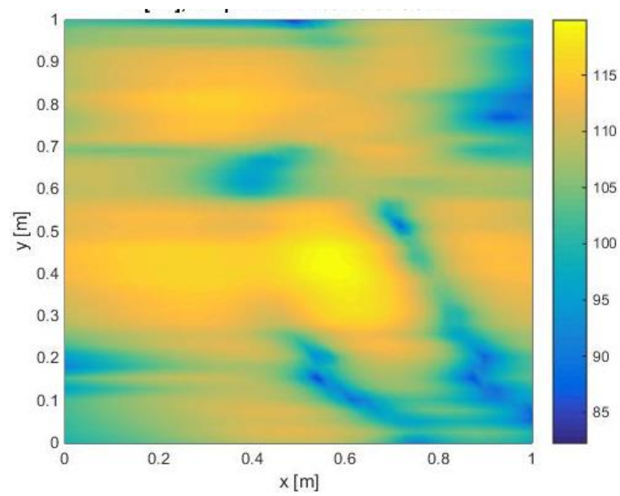

Fig. 11. The sound pressure level on the reconstruction plane with noise3, reconstructed using the SONAH general equation with manually chosen regularization parameter

As we can see, to estimate regularization parameter manually is not so trivial task. To properly chose the regularization parameter manually needed time and patience. But in this case, we can try and determine regularization parameter only because it is a simulation and we have the reference sound levels, that we can refer to understand if the way we are changing the regularization parameter is right. In real-world cases we usually don't have these references.

The other option how to determine the regularization parameter is to use Morozov discrepancy principle.

The Morozov algorithm in this simulation is solved this way:

```
s=1000000; %service variable
sigma1=sqrt(length(x)*length(y))*s1;
Hs=ones(length(x),length(y))*(j*w*p0);%spatial transfer function, made into
matrix
for ii=0:100
   eps=ii;
   ra=(inv(eps*eye(length(x))+(Hs')*Hs))*(Hs');
   P=Hs*ra*Pm; %wanted pressure matrix P from measured pressure
matrix Pm
   n=norm(P-Pm)-sigma1;
   if (n<s)
      s=n;
      eps_reg_meas0=ii;
   end
end
```

This algorithm is for noiseless data. For noisy data algorithm is the same, with one difference: matrix Pm is changed for pmeas_noise1, pmeas_noise2 or pmeas_noise3.

The results are the following:

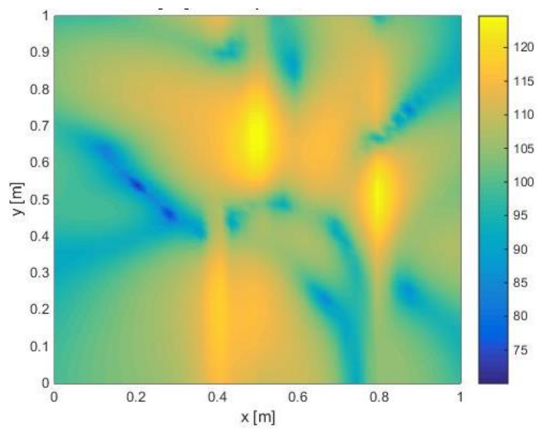

Fig. 12. The sound pressure level on the source plane, reconstructed using the SONAH general equation with Morozov method regularization parameter

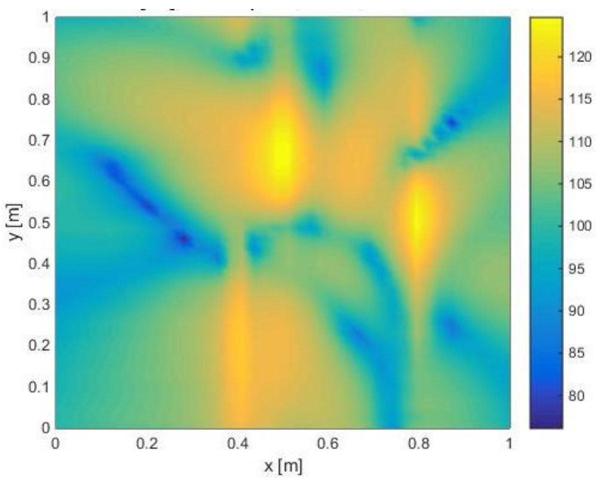

Fig. 13. The sound pressure level on the source plane with noise 1, reconstructed using the SONAH general equation with Morozov method regularization parameter

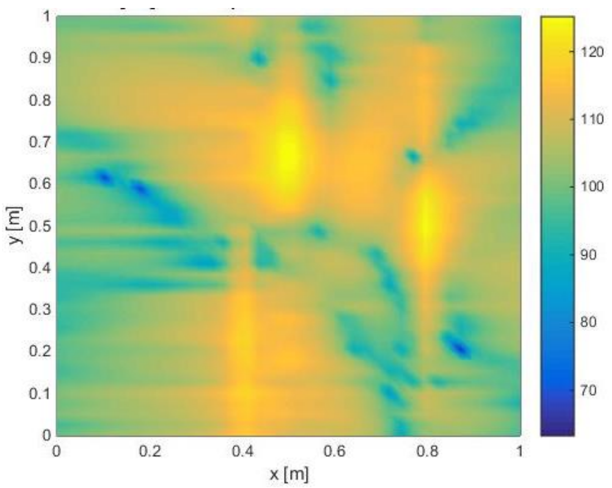

Fig. 14. The sound pressure level on the source plane with noise 2, reconstructed using the SONAH general equation with Morozov method regularization parameter

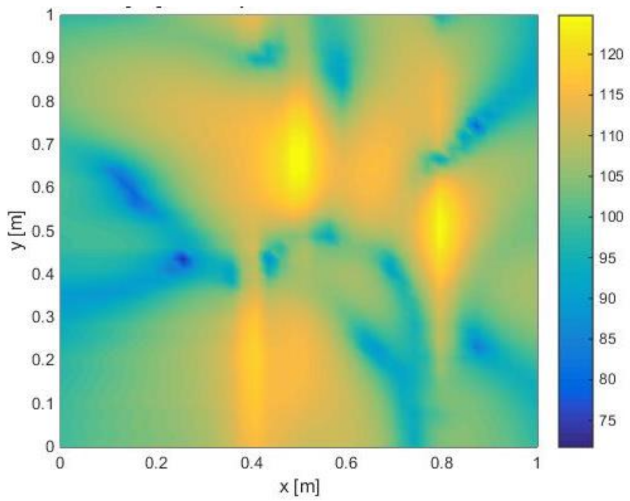

Fig. 15. The sound pressure level on the source plane with noise 3, reconstructed using the SONAH general equation with Morozov method regularization parameter

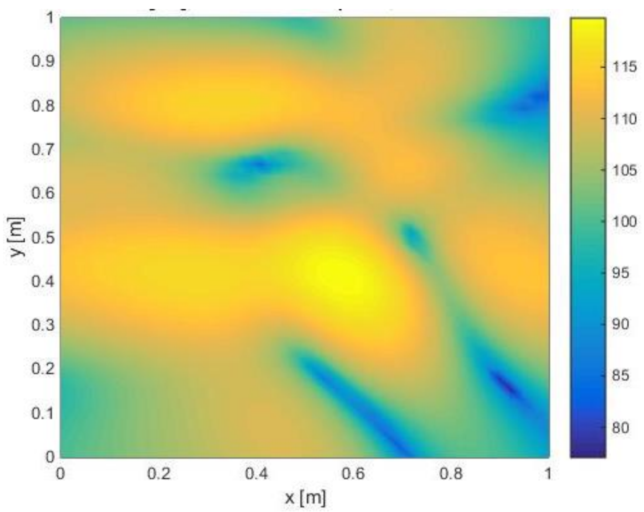

Fig. 16. The sound pressure level on the reconstruction plane, reconstructed using the SONAH general equation with Morozov method regularization parameter

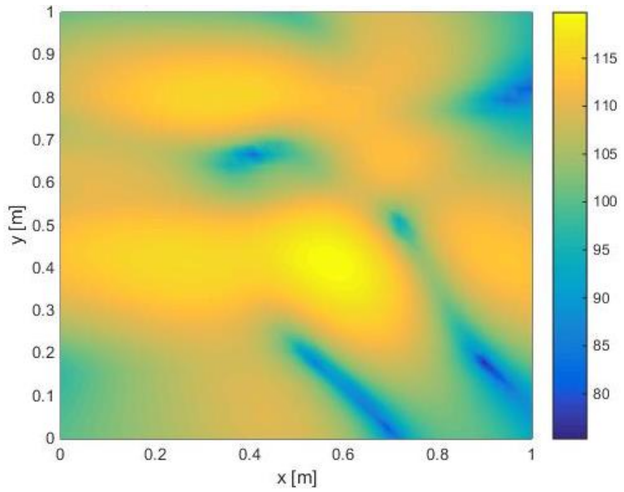

Fig. 17. The sound pressure level on the reconstruction plane with noise1, reconstructed using the SONAH general equation with Morozov method regularization parameter

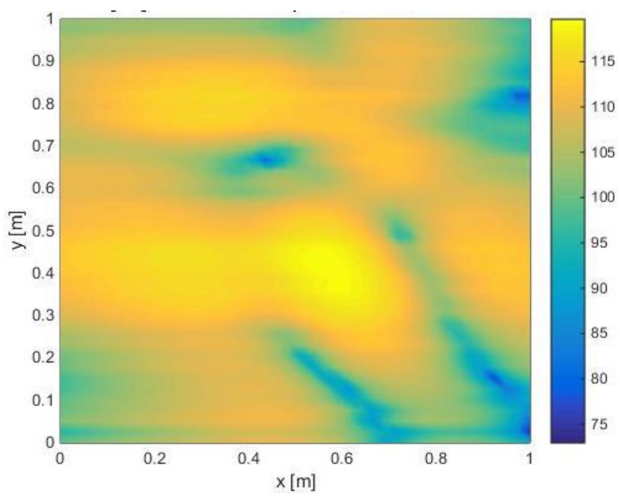

Fig. 18. The sound pressure level on the reconstruction plane with noise2, reconstructed using the SONAH general equation with Morozov method regularization parameter

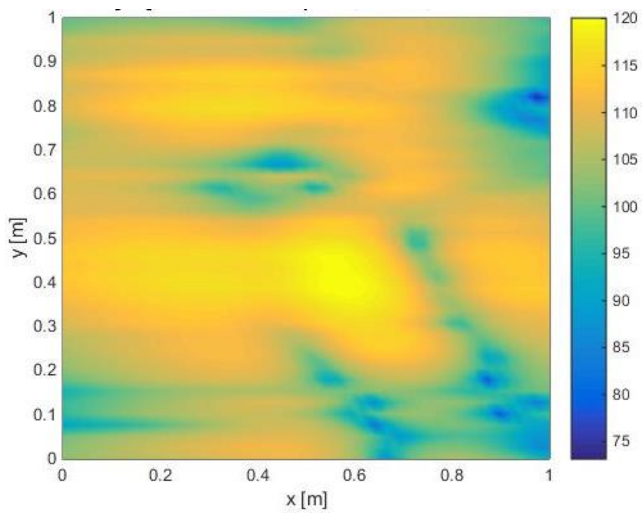

Fig. 19. The sound pressure level on the reconstruction plane with noise3, reconstructed using the SONAH general equation with Morozov method regularization parameter

The regularization parameter in these cases was 30, for all eight reconstructions. As we can see, the results of both regularization technics are almost the same, but for Morozov algorithm we weren’t using the verifying images.

4. Conclusion

In this bachelor thesis were briefly reviewed main three methods of the NAH: the Fourier-based Near-field acoustic holography method (also referred as a general NAH), Statistically Optimized Near-field Acoustic Holography (SONAH) and Helmholtz Equation Least-Square method (HELS).

The SONAH method with Tikhonov regularization was simulated in this thesis with results presented in figures in previous part. Studying resulting images, we can conclude, that with increasing noise variance and power, the quality of the obtained hologram decreases. Acoustic holography methods are designed for getting out of the noisy data the results as free of noise influence as possible.

For the determination of the regularization parameter two methods were used: manually chosen value and Morozov method. Even thought in the end images for the same initial conditions looks almost the same, the amount of time, need for these results, is different. The Morozov method, if programmed right, takes far less time for returning the satisfying result, while with manually chosen value of the regularization parameter there is a need to restart algorithm several times to finally find the satisfying image.

The next steep, in continuation of this thesis, could be the simulation of the next acoustic holography methods and regularization technics, or comparison the results of the simulations to the results of the real measurement.

The Near-field Acoustic Holography is a rapidly progressing field of the acoustic measurement. The methods of Near-field Acoustic Holography are constantly developing and so are the regularization technics. The main field of application of the acoustic holography methods is a localization of the sources of the vibration.

5. Bibliography

[1] Jaud, V.: Particle Velocity-based Statistically Optimised Nearfield Acoustic Holography. Master Thesis. Acoustic Technology, Danish Technical University, 2006.

[2] Hald, J.: Basic theory and properties of statistically optimized near-field acoustical holography. The Journal of the Acoustical Society of America 125(4), 2105- 2120, 2009.

[3] Havránek, Z.: Using Acoustic Holography for Vibration Analysis. Doctoral Thesis. Department of control and instrumentation, Brno University of Technology, 2009.

[4] Koutný, A.: Sound Source Localization in Enclosures, Doctoral Thesis, Department Physics, Faculty of Electrical Engineering, Czech Technical University in Prague, 2017.

[5] Koutný, A., Švec, P.: Porovnání regularizačních metod v akustické holografii a volba optimálních parametrů. 80.akustický seminář, České Vysoké Učení Technické v Praze, Česká akustická společnost, 4-6 May, 2010.

[6] Mokhtari, M., Lopez Arteaga, I., Aangenent, W. H. T. M.: Vibration detection using Fourier acoustics. Department of Mechanical Engineering, Eindhoven University of Technology. D&C; Vol. 2011.007, 2011.

[7] Qian, Q., Hang, C., Biao, Z., Jinxiang, D., Hu Y.: Sound Field Holographic Reconstruction System Based on Nearfield Acoustic Holography. IEEE International Conference on Signal Processing, Communications and Computing (ICSPCC), 5-8 August 2016.

[8] Wang, Z., Wu, S.F.: Helmholtz equation–least-squares method for reconstructing the acoustic pressure field. The Journal of the Acoustical Society of America, 102(4), 2020-2032, 1997.

[9] Williams, E. G.: Fourier Acoustics, Sound Radiation and Nearfield Acoustical Holography, Academic Press, 1999.

[10] Williams, E.G.: Regularization methods for near-field acoustical holography. The Journal of the Acoustical Society of America ,110(4), 1976-1988, 2001.